Highly sensitive electrochemical biosensor based on nonlinear hybridization chain reaction for DNA detection

Liping Jia, Shanshan Shi, Rongna Ma, Wenli Jia, Huaisheng Wang

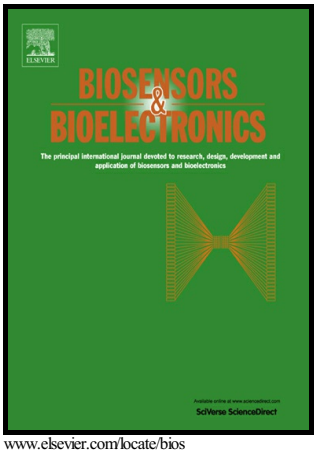

www.elsevier.com/locate/bios

PII: S0956-5663(16)30114-2
DOI: http://dx.doi.org/10.1016/j.bios.2016.02.007
Reference: BIOS8439

To appear in: *Biosensors and Bioelectronic*

Received date: 9 December 2015
Revised date: 19 January 2016
Accepted date: 2 February 2016

Cite this article as: Liping Jia, Shanshan Shi, Rongna Ma, Wenli Jia and Huaisheng Wang, Highly sensitive electrochemical biosensor based on nonlinear hybridization chain reaction for DNA detection, *Biosensors and Bioelectronic* http://dx.doi.org/10.1016/j.bios.2016.02.007

Highly sensitive electrochemical biosensor based on nonlinear hybridization chain reaction for DNA detection

Liping Jia, Shanshan Shi, Rongna Ma, Wenli Jia, Huaisheng Wang*

Department of Chemistry, Liaocheng University, Liaocheng 252059, China

*Corresponding author. Tel: +86-635-8239121; Fax: +86-635-8239121.

E-mail address: hswang@lcu.edu.cn

Abstract:

In the present work we demonstrated an ultrasensitive detection platform for specific DNA based on nonlinear hybridization chain reaction (HCR) by triggering chain-branching growth of DNA dendrimers. HCR was initiated by target DNA (tDNA) and finally formed dendritic structure by self-assembly. The electrochemical signal was drastically enhanced by capturing multiple catalytic peroxidase with high-ordered growth. Electrochemical signals were obtained by measuring the reduction current of oxidized 3, 3′, 5, 5′-tetramethylbenzidine sulfate (TMB), which was generated by HRP in the presence of H_2O_2. This method exhibited ultrahigh sensitivity to tDNA with detection limit of 0.4 fM. Furthermore, the biosensor was also capable of discriminating single-nucleotide difference among concomitant DNA sequences.

Keywords: Biosensor, DNA, Nonlinear hybridization chain reaction

1. Introduction

The detection of sequence-specific DNA has recently attracted much attention due to its diverse applications including the identification of genetic diseases, disorders, the detection and characterization of viruses, bacteria, and parasites (Zhang et al., 2008; Wang et al., 2015). Recently, numerous methods including fluorescence (Zuo er al., 2010; Huang et al., 2012; Guo et al., 2013), electrochemistry (Zhu et al., 2013; Liu et al., 2013), electrochemiluminescence (Zhang et al., 2013; Zhou et al., 2012a; Zhou et al., 2012b), chemiluminescence (Willner et al., 2008; Weizmann et al., 2006), quartz-crystal microbalance (Wang et al., 2013), and surface plasmon resonance

technique (Wood et al., 2013; Mousavi et al., 2013) have been used for the detection of sequence-specific DNA. In the above methods, electrochemical biosensors are much popular because of their simple instrumentation setup, low sample and reagent consumption as well as high sensitivity and selectivity (Wen et al., 2012; Lu et al., 2012; Wen et al., 2011; Farjami et al., 2011; Xia et al., 2010; Xiang and Lu, 2012; Pei et al., 2011; Farjami et al., 2013; Liu et al., 2013).

However, a challenge in electrochemical biosensor design is the efficiency of signal amplification and the sensitivity. In order to improve the sensitivity, a number of amplification strategies have been developed, including polymerase chain reaction (PCR) (Mullis and Faloona, 1987), rolling circle amplification (RCA) (Liu et al., 1996), strand-displacement amplification (SDA) (Walker et al., 1992) and hybridization chain reaction (HCR) (Zhang et al., 2015; Hou et al., 2015). HCR was firstly introduced as a signal amplification strategy by Dirks and Pierce in 2004 (Dirks et al., 2004). This method provides a general principle to initiate the successive assembly of DNA hairpins into nicked polymeric nanowires by the introduction of a triggering sequence. This technique of signal amplification proceeds at room temperature without the use of enzymes and does not require a thermal cycler, thereby eradicates the problems associated with PCR (Ikbal et al., 2015). Theoretically, the concept of HCR is not limited to linear polymerization of DNA hairpins. It can be extended to the programming of more complicated DNA hairpin sets that can assemble into branched or even dendritic structure under a triggered process, realizing nonlinear HCR systems that exhibit exponential growth (Xuan and Hsing, 2014). However, at present most electrochemical biosensors were fabricated based on the linear polymerization of DNA due to the complexity of sequence design for nonlinear growth (Chen et al., 2011; Ge et al., 2014).

Here we present an ultrasensitive detection platform for specific DNA based on hairpin-free nonlinear HCR by triggering chain-branching growth of DNA dendrimers (Scheme 1). HCR was initiated by tDNA and finally formed dendritic structure by introducing two hybridization DNA chain (H1 and H2). The biotin labeled H1 was used to capture avidin-modified peroxidase (avidin-HRP) via the strong biotin-avidin

interaction. A large number of HRPs were attached on the dendritic DNA chains by HCR, which amplified the final electrochemical signal. This method exhibited ultrahigh sensitivity to tDNA with detection limit of 0.4 fM. Furthermore, the biosensor was also capable of discriminating single-nucleotide difference among concomitant DNA sequences.

2. Experimental

2.1 Chemical and Reagents

All oligonucleotides were synthesized and purified by Sangon Biotech Co., Ltd. (Shanghai, China), and the base sequences are shown in Table S1. Tris-(2-carboxyethyl)-phosphine hydrochloride (TCEP), tris-(hydroxymethyl)-aminomethane, 6-mercapto-1-hexanol (MCH), and avidin-peroxidase (avidin-HRP) were purchased from Sigma-Aldrich. Ethylenediaminetetraacetic acid (EDTA) and 3, 3', 5, 5'-tetramethylbenzidine dihydrochloride (TMB-HCl) were purchased from Aladdin Inc. (Shanghai, China). All reagents were of analytical grade and without further purification. Double distilled water was used in the whole experimental process.

2.2 Measurements and apparatus

All electrochemical measurements were performed on a CHI760 electrochemical workstation (Shanghai, China) with a conventional three-electrode system composed of a platinum auxiliary electrode, an Ag/AgCl (3M KCl) reference electrode, and a gold working electrode. Amperometric detection was performed in a 5 mL 0.1 M (pH 7.0) phosphate buffer solution containing 0.15 mM TMB and 0.2 mM H_2O_2 at the potential of 150 mV, and the electroreduction current was measured 100 s after the HRP redox reaction reached steady. The electrochemical impedance spectroscopy (EIS) measurements were carried out in a background solution of 20 mM $[Fe(CN)_6]^{3-/4-}$ containing 0.1 M KCl with a frequency range from 0.1 Hz to 100 kHz. The amplitude of the applied sine wave potential was 5 mV and the formal potential of the system was set at +0.22 V.

UV–Vis absorption spectra were obtained using a Shimadzu UV-2550 spectrophotometer.

2.3 Preparation of biosensors

All oligo DNA were dissolved in Tris-HCl buffer (25 mM Tris-base, 100 mM NaCl and 10 mM $MgCl_2$, pH 7.4). Firstly, the mixture of capture DNA (CP) and auxiliary DNA1 (A1) solutions (1:1.5) was heated to 90℃ for 5 min and then allowed to cool on ice for 15 min, subsequently placed for 20 minutes at room temperature to form a double-stranded substrate. Finally the mixture was incubated with 1 mM TCEP for 1 h to reduce disulfide bonds. Excess A1 was added to make sure that all of the CP was protected.

The biotin- labeled hybridization DNA1 (H1) solution was mixed with avidin-HRP solution (1 ： 1) for 30 min to form HRP-labeled H1 (noted as HRP-H1).

The gold electrode was polished with 1.0, 0.3 and 0.05 μm alumina slurry sequentially, and rinsed thoroughly with ultrapure water between each polishing step. Next, the electrode was ultrasonically cleaned in ethanol and ultrapure water for 10 min successively. Finally, the electrode was electrochemically activated in 0.5 M H_2SO_4 until a stable cyclic voltammogram was obtained. After being dried with pure nitrogen gas, the electrode was immediately used for the DNA immobilization. The cleaned gold electrode was soaked in 50 μL 0.1 μM double-stranded substrate solutions for 2 h at room temperature. Then the electrode was thoroughly rinsed with PBS buffer. After drying with nitrogen, the electrode was immersed in 0.1 μM MCH solution for 1 h to remove the nonspecific DNA adsorption. Then the double-stranded substrate modified electrode was incubated with 50 μL hybridization solution (25 mM Tris, 100 mM NaCl, 10 mM $MgCl_2$, pH 7.4) containing different concentrations of tDNA for 2 h at room temperature. The resulted electrode was incubated in 0.1 μM auxiliary DNA2 (A2) solutions for 2 h at room temperature. Afterward, the HCR was carried out by alternately immersing the modified electrode in 0.5 μM HRP-labeled hybridization DNA1 (HRP-H1) solution and 0.5 μM hybridization DNA2 (H2) solutions for 30 min at room temperature. Between every two self-assembly steps, the

electrode was washed with hybridization solutions and dried with nitrogen gas.

3. Results and discussion

3.1 Design principle of the biosensor

The design principle of the proposed biosensor for sequence-specific DNA detection is schematically illustrated in scheme 1. Five components such as 3′-thiol-modified capture DNA (CP), auxiliary DNA1 (A1), auxiliary DNA2 (A2), HRP-labeled hybridization DNA1 (HRP-H1) and hybridization DNA2 (H2) were employed in this work. First, the CP hybridized with complementary region of A1, forming an exposed "toehold" at one end and two bulge loops in the middle. Then, the formed double-stranded substrate was immobilized on the gold electrode via Au-S bond. When tDNA was introduced, it hybridized and docked to the exposed toehold of CP, which displaced part of A1 and opened the first loop. Next the A2 completely complementary with A1 spontaneously hybridized to A1, which made A1 away from CP and opened the second loop. The opened loops exposed the displaced part of the A1 as a new toehold and launched the branch growth. Now the CP exposed two identical sequences connected in series, which could simultaneously be attacked by and hybridized with two HRP-H1. And then there were two new exposed "toeholds" at end of each HRP-H1 strand formed again. Following two H2 hybridized with the "toeholds" respectively and each of them left two identical sequences that complementary to HRP-H1, which was ready to enter a new round of reactions. In this way a sustainable chain-branching process began. Theoretically this chain-branching growth of the dendritic structure would sustainably continue, and a DNA dendrimer with 2^n exposed HRP could be formed after n reaction cycles. Thus the final electrochemical signal will be greatly amplified.

Scheme 1.

3.2 Characterization of the biosensor

As control tests, the electrochemical characteristics of the electrodes after each step were investigated by using electrochemical impedance spectroscopy (EIS) (Fig. 1).

$[Fe(CN)_6]^{3-/4-}$ couple was employed as the electrochemical redox probe for EIS measurements, while the Nyquist plots were utilized to calculate the electron-transfer resistance. A very small semicircle was observed for bare gold electrode (curve a), indicating a low electron-transfer resistance. In contrast, the resistance increased when the double-stranded substrate was assembled on the gold electrode (curve b). The reason was ascribed to the electrostatic repulsion between the phosphate backbone of DNA and the negatively charged $[Fe(CN)_6]^{3-/4-}$ ions. The electron-transfer resistance continued to increase (curve c and d) with the introducing of tDNA and A2 sequentially. Especially after 5 hybridization chain reaction cycles with H1 and H2, the resistance drastically increased (curve e). This may be attributed to the facts: (1) DNA molecules immobilized on the electrode got more and more with the hybridization reaction cycles increasing, which resulted in the stronger electrostatic repulsion; (2) the space steric effect of the formed dendrimer structures made the electron transfer of $[Fe(CN)_6]^{3-/4-}$ more difficult.

Fig. 1

To clarify whether H1 and H2 could be non-specifically assembled to the electrode, the electrochemical characteristics of the prepared sensors were studied by amperometric response through a series of control experiments (Fig. 2A). In the present work the catalytic current could be detected by reducing the oxidation product of 3, 3', 5, 5'-tetramethylbenzidine (TMB), which was oxidized by the HRP on the electrode surface in the presence of H_2O_2. As shown in Fig. 2A, there was weak electrocatalytic current produced in the absence of tDNA. However, in the presence of tDNA (0.1 μM), we can observe an apparent increase in current from I−t curve. And the current (5.8 μA) is about 120 times higher than that (~47 nA) without tDNA. This relatively large difference makes our detection sensitive.

In order to further verify the sensor's feasibility, we used UV-Vis spectra to measure whether the electrocatalytic reaction happened. As is known to all that TMB solution exhibits no color and the oxidized TMB solution shows obvious blue color (Chen et al., 2011). We also found that the solution was still colorless when the biosensor fabricated in the absence of tDNA placed in the PBS containing TMB and

H_2O_2. However, when the biosensor fabricated in the presence of 0.1 μM tDNA placed in the above solution, it slowly changed to bluish. As shown in Fig. 2B, the solution shows no absorption peaks in the wavelength range from 260 to 700 nm (curve black) in the absence of tDNA. However, three strong absorption peaks appear at 370 nm, 457 nm and 650 nm respectively in the presence of 0.1 μM tDNA, which are attributed to the oxidation of TMB by HRP immobilized on the electrode surface in the presence of H_2O_2. It also indicates the self-assembly can be performed only in the presence of tDNA. The above results show that the prepared biosensor is feasible.

Fig. 2

3.3 Optimization of hybridization chain reaction cycles

In the absence of steric effect, theoretically this chain-branching growth of the dendritic structure would continue, and a DNA dendrimer with 2^n exposed HRP could be formed after n reaction cycles. Concurrently, the electrocatalytic current of TMB would also increase exponentially. So we investigated the changes of reduction current of TMB with the increase of HCR cycles. As shown in Fig. 3, the currents of TMB first increased with the increase of HCR cycles, and then the currents tended to stable after 5 cycles. The results showed that the further chain reactions were hindered due to the steric effect.

Fig. 3

3.4 Detection of tDNA

Under the experimental conditions, the analytical performance of the fabricated sensing system was investigated. As shown in Fig. 4, the amperometric signal increased along with the increase of tDNA concentration, which indicated that the numbers of HRP immobilized on the electrode was highly dependent on the concentration of tDNA. The dynamic range of our detection spanned 5 orders of magnitude from 1 fM to 100 pM. A good linear correlation between the logarithm of the reduction current and the logarithm of tDNA concentration ranging from 1 fM to 1000 fM was obtained, with a correlation coefficient of R=0.9901. The detection

limit was estimated to be 0.4 fM based on S/N of 3. The comparison of our strategy with other reported HCR methods was illustrated in Table S2. Compared with most of conventional HCR-based DNA sensors, our strategy exhibited a relatively low detection limit and a wide linear range for the detection of target DNA. The satisfactory sensitivity of our biosensor may be ascribed to the high amplification efficiency based on nonlinear HCR and the sensitive electrochemical detection based on enzymatic reaction.

Fig. 4

The specificity of the DNA sensing system was further investigated using five DNA sequences, namely complete complementary target DNA, single-base mismatched, two-base mismatched DNA, five-base mismatched DNA and total mismatched DNA. As shown in Fig. 5, in the same concentration of DNA, the amperometric signals for single-base mismatched and two-base mismatched DNA were about 1.5 μA and 0.5 μA, which were obviously lower than that of the target DNA (6.3 μA). The five-base mismatched DNA and total mismatched DNA almost showed the same response with that of the blank solution. Therefore this method exhibited a good performance to discriminate perfect complementary target and the mismatched targets, and will be potential for single nucleotide analysis.

Fig. 5

The stability and reproducibility of the HCR-based DNA sensors were studied. The fabricated DNA sensor could be stored at 4℃ before use. After storage of one week, the current response could remain 91% of its initial value, indicating that the proposed sensor had acceptable stability. The reproducibility of HCR-based DNA sensors was examined by five repetitive measurements of 20 fM target DNA on a single electrode, which showed a relative standard deviation (RSD) of 5.1%. The RSD for three parallel DNA sensors fabricated on different electrodes was 8.4%.

4. Conclusion

In conclusion, we demonstrated an ultrasensitive detection platform for specific DNA based on nonlinear hybridization chain reaction (HCR) by triggering

chain-branching growth of DNA dendrimers. This dendrimer structure allowed multiple HRP enzymes to be captured, which amplified the final electrochemical signal through the catalytic reaction of H_2O_2. A wide linear range from 1 fm to1000 fm and a low detection limit of 0.4 fM toward target DNA could be achieved. Furthermore, the biosensor was also capable of discriminating single-nucleotide difference among concomitant DNA sequences. Moreover, this design strategy can be combined with other detection technology such as electrochemiluminescence, etc. So the developed ultrasensitive electrochemical DNA biosensor will have a great potential in the area of DNA diagnostics and clinical analysis.

Acknowledgements

This work is supported by the Natural Science Foundation of China (Nos. 21405070, 21075059, 21375055 & 21427808).

References

Chen, X., Lin, Y.H., Li, J., Lin, L.S., Chen, G.N., Yang, H.H., 2011. Chem. Commun. 47, 12116-12118.

Dirks, R.M., Pierce, N.A., 2004. Proc. Natl. Acad. Sci. U.S.A. 101, 15275-15278.

Farjami, E., Campos, R., Nielsen, J.S., Gothelf, K.V., Kjems, J., Ferapontova, E.E., 2013. Anal. Chem. 85, 121-128.

Farjami, E., Clima, L., Gothelf, K., Ferapontova, E.E., 2011. Anal. Chem. 83, 1594-1602.

Ge, Z.L., Lin, M.H., Wang. P., Pei. H., Yan. J., Shi, J.Y., Huang, Q., He, D.N., Fan, C.H., Zuo, X.L., 2014. Anal. Chem. 86, 2124-2130.

Guo, Y.H., Xu, P., Hu, H., Zhou, X.D., Hu, J.M., 2013. Talanta. 114, 138-142.

Hou, T., Li, W., Liu, X.J., Li, F., 2015. Anal. Chem. 87, 11368-11374.

Huang, J.H., Su, X.F., Li, Z.G., 2012. Anal. Biochem. 84, 5939-5943.

Ikbal, J., Lim, G.S., Gao. Z.Q., 2015. Trac-Trend Anal Chem. 64, 86-99.

Li, N., Hao, X., Kang, B.H., Xu, Z., Shi, Y., Lin, N.B., Luo, H.Q., 2016. Biosens. Bioelectron. 77, 525-529.

Liu, D., Daubendiek, S.L., Zillman, M.A., Ryan, K., Kool, E.T., 1996. J. Am. Chem. Soc. 118, 1587-1594.

Liu, S.F., Wang, C.F., Zhang, C.X., Wang, Y., Tang, B., 2013. Anal. Chem. 85, 2282-2288.

Liu, X.Q., Niazov-Elkan, A., Wang, F.A., Willner, I., 2013. Nano Lett. 13, 219-225.

Liu, Y.F, Luo, M., Yan, J., Xiang, X., Ji, X.H., Zhou, G.H., He, Z.K., 2013. Chem. Commun. 49, 7424-7426.

Lu, N., Pei, H., Ge, Z.L., Simmons, C.R., Yan, H., Fan, C.H., 2012. J. Am. Chem. Soc. 134, 13148-13151.

Mousavi, M.Z., Chen, H.Y., Wu, S.H., Peng, S.W., Lee, K.L., Wei, P.K., Cheng, J.Y., 2013. Analyst. 138, 2740-2748.

Mullis, K.B., Faloona, F.A., 1987. Methods Enzymol. 155, 335-350.

Pei, H., Wan, Y., Li, J., Hu, H.Y., Su, Y., Huang, Q., Fan, C.H., 2011. Chem. Commun. 47, 6254-6256.

Walker, G.T., Little, M.C., Nadeau, J.G., ShankProc, D.D., 1992. Proc. Natl. Acad. Sci. USA. 89, 392-396.

Wang, Cui., Zhou, H., Zhu, W.P., Li, H.B., Jiang, J.H., Shen, G.L., Yu, R.Q., 2013. Biosens. Bioelectron. 47, 324-328.

Wang, J., Zhu, Z., Ma, H., 2013. Anal. Chem. 85, 2096-2101.

Wang, X.Z., Ge, L., Yu, Y.F., Dong, S.S., Li, F., 2015. Sens. Actuators B. 220, 942-948.Weizmann, Y., Beissenhirtz, M.K., Cheglakov, Z., Nowarski, R., Kotler, M., Willner, I., 2006. Angew. Chem. Int. Ed. 45, 7384-7388.

Wen, Y. L., Pei, H., Shen, Y., Xi, J. J., Lin, M. H., Lu, N., Shen, X.Z., Li, J., Fan, C.H., 2012. Sci. Rep. 2, 867-873.

Wen, Y.L., Pei, H., Wan, Y., Su, Y., Huang, Q., Song, S.P., Fan, C.H., 2011. Anal. Chem. 83, 7418-7423.

Willner, I., Shlyahovsky, B., Zayats, M., Willner, B., 2008. Chem. Soc. Rev. 37, 1153-1165.

Wood, J.B., Szyndler, M.W., Halpern, A.R., Cho, K., Corn, R.M., 2013. Langmuir. 29, 10868-10873.

Xia, F., Zuo, X.L., Yang, R.Q., Xiao, Y., Kang, D., ValleeBelisle, A., Gong, X., Heeger, A.J., Plaxco, K.W., 2010. J. Am. Chem. Soc. 132, 1252-1254.

Xiang, Y., Lu, Y., 2012. Anal. Chem. 84, 4174-4178.

Xuan, F., Hsing, I.M., 2014. J. Am. Chem. Soc. 136, 9810-9813.

Yu, X., Zhang, Z.L., Zheng, S.Y., 2015a. Biosens. Bioelectron. 66, 520-526.

Yu, Y.Y., Chen, Z.G., Jian, W.S., Sun, D.P., Zhang, B.B., Li, X.C., Yao, M.C., 2015b. Biosens. Bioelectron. 64, 566-571.

Zhang, B., Chen, J., Liu, B., Tang, D., 2015. Biosens. Bioelectron. 69, 230-234.

Zhang, F., Chen, H., He, P.G., Fang, Y.Z., 2013. Chin. J. Anal. Chem. 41, 1-9.

Zhang, J., Qi, H.L., Li, Y., Yang, J., Gao, Q., Zhang, C.X., 2008. Anal. Chem. 80, 2888-2894.

Zhao, J.J., Chu, Z.D., Jin, X., Zhao, S.L., 2015. Sens. Actuators B. 209, 116-121.

Zhou, H., Zhang, Y.Y., Liu, J., Xu, J.J., Chen, H.Y., 2012a. J. Phys. Chem. C. 116, 17773-17780.

Zhou, X.M., Xing, D., 2012b. Analyst. 137, 4188-4192.

Zhu, Z., Lei, J.P., Liu, L., Ju, H.X., 2013. Analyst. 138, 5995-6000.

Zuo, X.L., Xia, F., Xiao, Y., Plaxco, K.W., 2010. J. Am. Chem. Soc. 132, 1816-1818.

Figure captions:

Fig. 1. EIS Nyquist plots for (a) bare gold electrode, (b) electrode（a)+ CP+A1+MCH, (c) electrode (b)+tDNA, (d) electrode (c)+A2, and (e) electrode (d)+H1+H2 (5 cycles).

Fig. 2. (A) Amperometric response of TMB on the prepared DNA dendrimer-based sensor in the presence of 0 μM and 0.1 μM tDNA. The potential was held at 150 mV (vs Ag/AgCl). (B) UV-Vis absorption spectra of TMB in the presence of 0 μM and 0.1

μM tDNA.

Fig. 3. (A) Amperometric response of TMB for different reaction cycles. (B) Linear curve of reduction currents vs. cycles. Error bars show the standard deviations of measurements taken from three tests.

Fig. 4. (A) The amperometric response of the sensor to different concentrations of target DNA. (a) 0 fM, (b) 1 fM, (c) 10 fM, (d)100 fM, (e) 1 pM, (f) 10 pM and (g) 100 pM. (B) Calibration curve between the amperometric currents and tDNA concentrations. Inset shows the linear relationship between the logarithm of current and the logarithm of the tDNA concentration. Error bars show the standard deviations of measurements taken from three tests.

Fig. 5. (A) and (B) Comparison of the amperometric signals for the prepared DNA sensor in the presence of same concentration complementary target DNA (a), single-base mismatched DNA (b), two-bases mismatched DNA (c), five-bases mismatched DNA (d), total mismatched DNA (e) and in the absence of target DNA (f). Error bars show the standard deviations of measurements taken from three tests.

Scheme 1. Schematic illustration of the designed biosensor. DNA sequences drawn in the same color are either identical or complementary.

Fig. 1

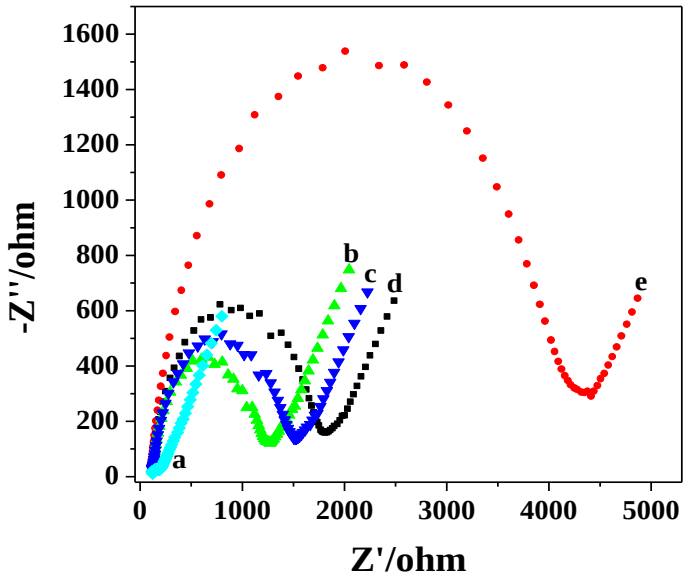

Fig. 2

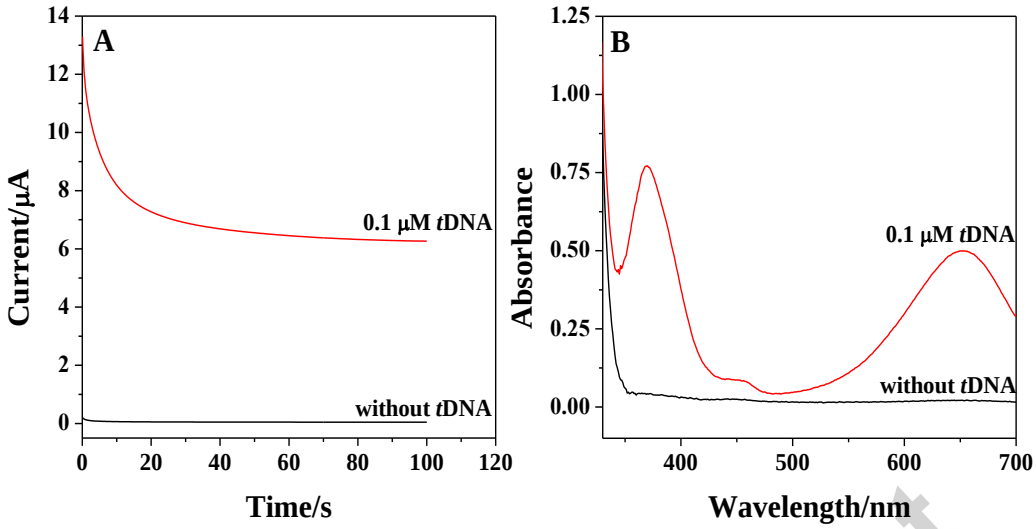

Fig. 3

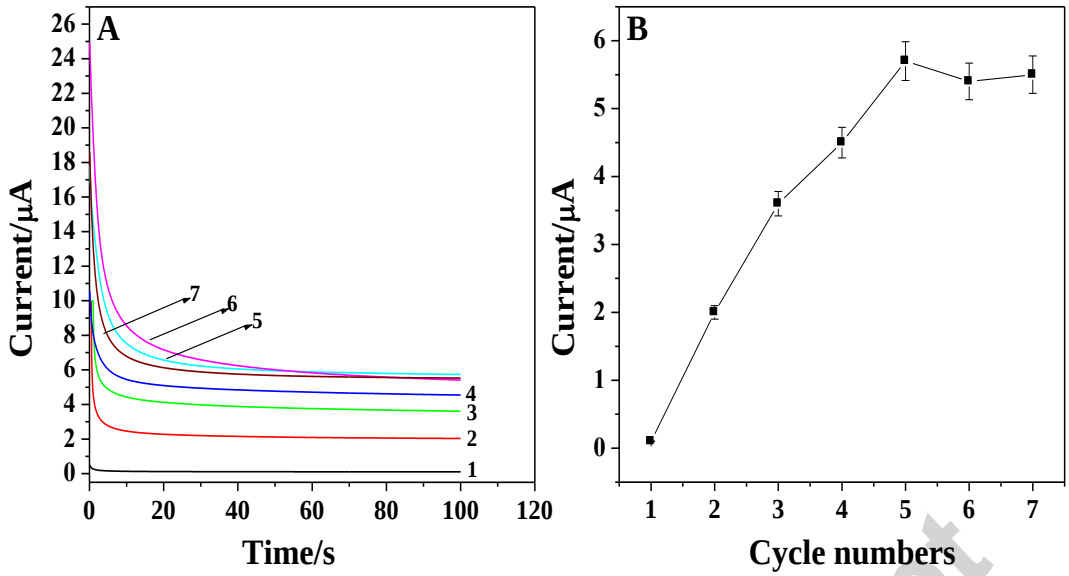

Fig. 4

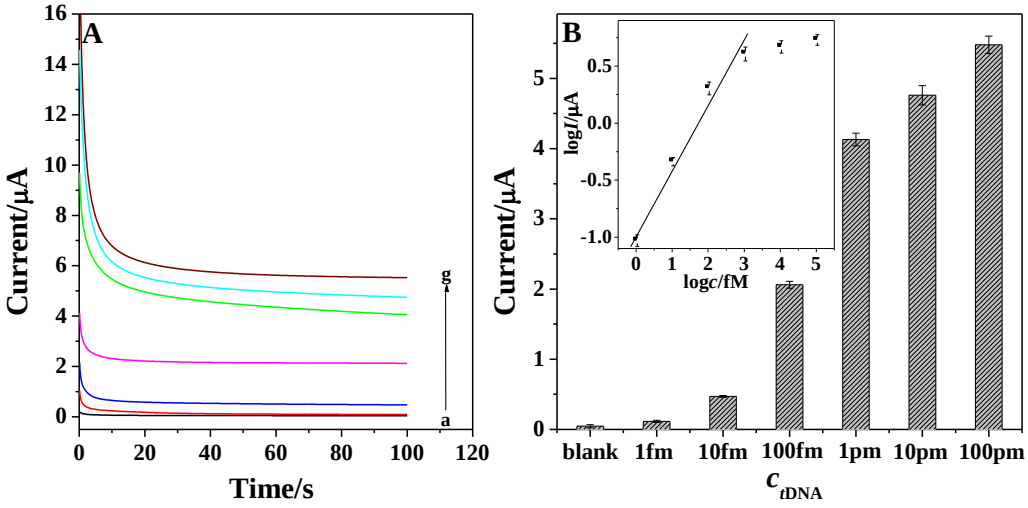

Fig. 5

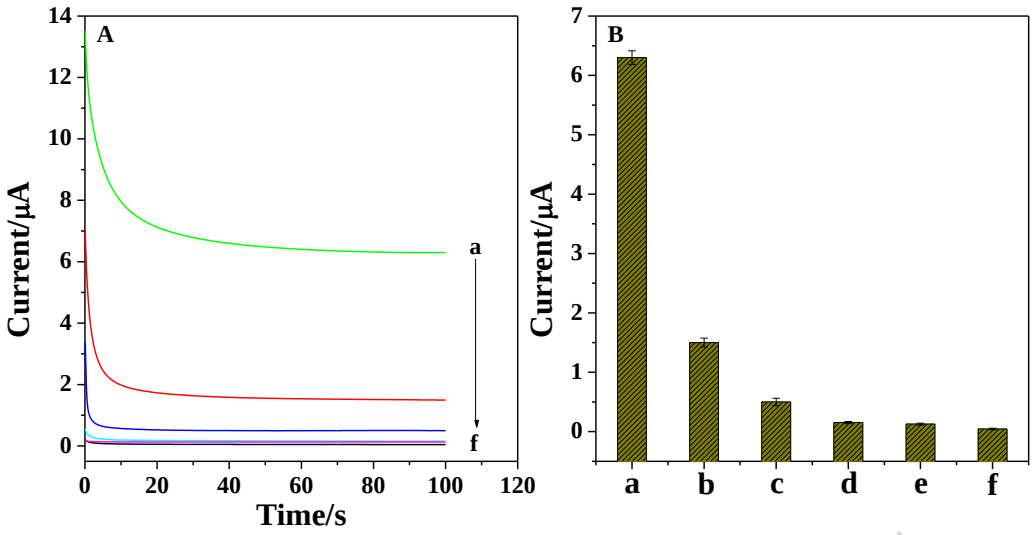

Scheme 1

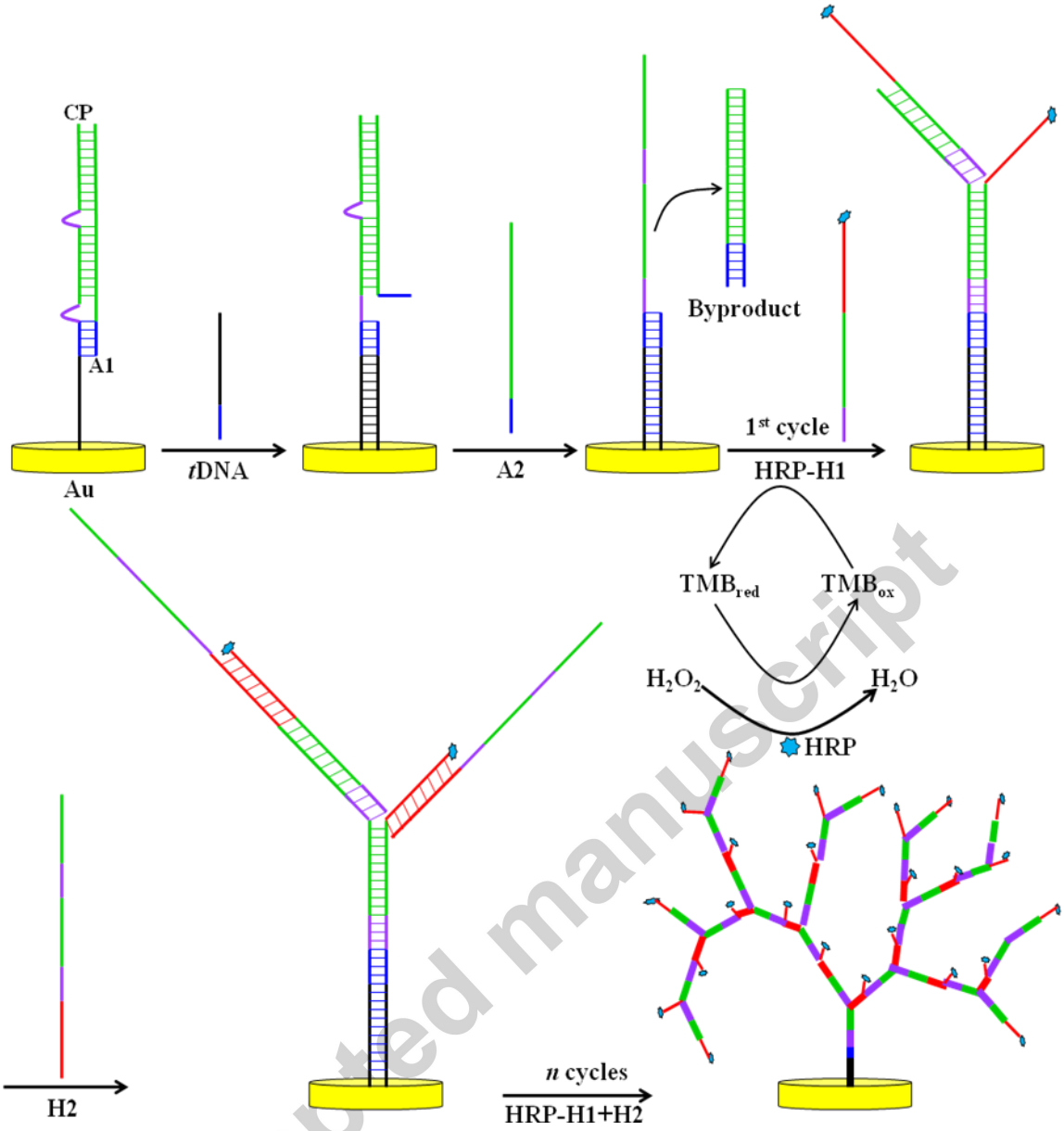

Highlight:

- We develop a novel nonlinear hybridization chain reaction for the detection of DNA.
- A dendritic structures was formed by nonlinear hybridization chain reaction via triggering chain-branching growth of DNA.
- The proposed method showed good sequence specificity for tDNA recognition